07

Optoelectronic reservoir computing system with output layer modification

© G.O. Danilenko, D.A. Pavlov, E.A. Viktorov, A.V. Kovalev

ITMO University, St. Petersburg, Russia
E-mail: avkovalev@itmo.ru

Received April 16, 2025
Revised June 8, 2025
Accepted June 9, 2025

A reservoir computing system based on a vertical-cavity surface emitting laser with optoelectronic feedback has been studied experimentally. The paper demonstrates how the output layer configuration influences the accuracy of solving the task of predicting the Santa Fe chaotic time series.

Keywords: reservoir computing, semiconductor lasers, optoelectronic feedback, machine learning.

DOI: 10.61011/TPL.2025.09.61815.20345

Currently, active search and research are being performed into new computing paradigms including those involving dynamic processes in analog physical systems. Among the latters, that to be separately distinguished is reservoir computing (RC) based on a nonlinear delayed-feedback (FB) device, which is an analogue of a recurrent neural network [1–3] organized by time multiplexing with formation of so-called virtual nodes. The delayed-FB RC systems have been implemented by using devices of the optical [4], electronic [5], memristor [6], spin-wave [7] and other types [8].

Physical implementation of RC based on optoelectronic devices is an important research and technological issue whose solution may provide high-speed and energy-efficient data processing systems. Previously, study [9] has experimentally demonstrated an RC system based on a semiconductor laser with delayed optoelectronic feedback (OEFB) that was theoretically investigated in [10–12]. The system employs a nonlinear response arising due to excitation of laser relaxation oscillations in case the system is perturbed and its parameters are in the vicinity of the Andronov–Hopf bifurcation. Experimental paper [13] considers a similar reservoir computing system based on nonlinearity of the semiconductor laser I-V characteristic and long-delay OEFB not using the fast dynamics of laser response.

In [9] there were observed limitations of the data processing efficiency caused by relatively narrow bandwidths of the laser modulation and OEFB transmission. The system operation principle is time multiplexing of virtual nodes, which makes it important to increase the system modulation bandwidth in order to improve the quality of computational problems' solutions. This paper presents a reservoir computing system based on a vertical-cavity semiconductor laser (VCSEL) with a high pump current modulation frequency and improved OEFB loop comprising a semiconductor optical amplifier and electronic path with an FB transmission bandwidth which is more uniform and wider due to using an equalizer and broadband electronic signal amplifiers. This allows using a larger number of virtual nodes in solving complex machine learning problems, e.g. predicting the Santa Fe chaotic time series [14].

The RC specific feature is simplification of the learning process as compared to neural networks of other types, since in the process of learning only the output layer weighting factors to be determined by linear regression are subject to adjustment. In [15] it was theoretically shown that the accuracy of solving the problem of predicting time series by the RC system may be increased by using in the output layer, in addition to the RC system node states, their squared values. This paper demonstrates, based on experimental data, the effect of the output layer organization method on the accuracy of the solution to the problem of predicting the Santa Fe chaotic time series, and proposes a new procedure for processing the node state values.

Experimental setup for the optoelectronic RC system is schematically represented in Fig. 1, *a*. All the optical components are interconnected via conventional single-mode fiber with FC-connectors, while electronic components are interconnected using coaxial cable assemblies with SMA connectors. The system includes a VCSEL module with SMA-connector and fiber tail (VCSEL, „OKB Planeta“, wavelength 1550 nm, threshold pump current 1.5 mA, output radiation power 0.25 mW at 3 mA, modulation bandwidth 8 GHz at the level of −3 dB). The laser was pumped by stabilized current source Keysight N6705C (CS). The VCSEL output radiation passes through an isolator (OI) and polarization controller (PC) and is fed to the semiconductor optical amplifier (SOA, JSC „Nolatex“) pumped and temperature-controlled by the Nordlase NLDCW-2000-HPR driver (SD) in order to increase power of the optical signal recorded by photodetector (PD) Alphalas UPD-15-IR2-FC having sensitivity of 24 mV/mW for the wavelength of 1550 nm in operating on a matched load of 50 Ω (corresponds to 0.48 A/W). The SOA transparency current (corresponding to gain of 0 dB) in operation with VCSEL is 72 mA. SOA exhibits a nearly linear gain dependence on current with the proportionality coefficient of 0.38 dB/mA in the range of 72–90 mA. Isolators OI

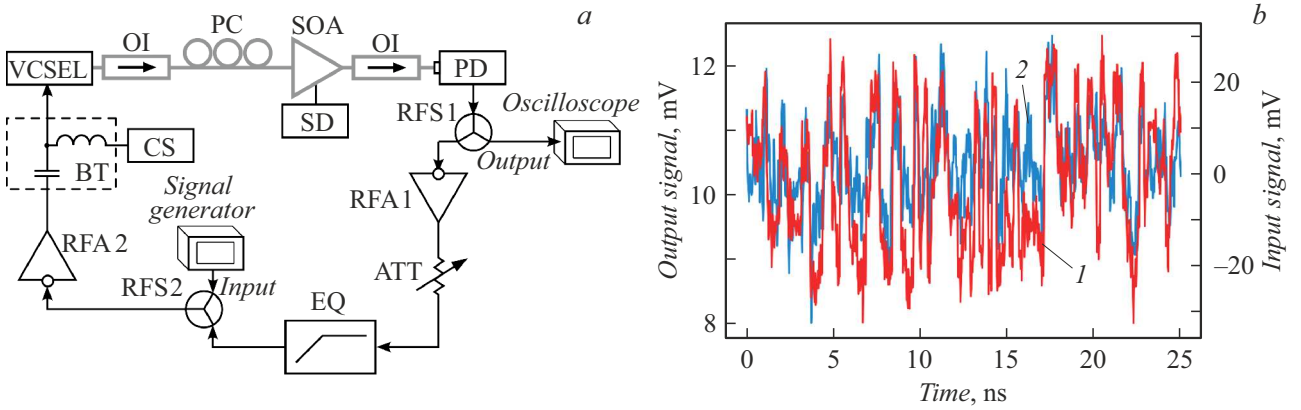

Figure 1. *a* — schematic diagram of an optoelectronic reservoir computing system based on VCSEL and semiconductor optical amplifier. Grey lines represent the optical signal; black lines are for the electrical signal. *b* — a case of timing diagrams of the input (*1*) and output (*2*) signal at the system parameters given in the Table for the virtual nodes number of 100. For clarity, the input signal is inverted, since prior to be fed to VCSEL it passes through inverting RFA 2. The color version of the figure is presented in the electronic version of the article.

are used to prevent the effect of parasitic optical feedback on the laser and SOA self-excitation. A portion of the PD output electrical signal is fed through power divider SHWLPD2-DC12S (RFS 1, bandwidth 0–12 GHz) to the Keysight UXR0204A oscilloscope in order to record the PD signal timing diagrams and fix values of the RC system node states; another portion is fed into the FB-loop electronic path. The procedure for recording the node state values with an oscilloscope is described in detail in [9]. To reduce the effect of noise, timing diagrams recorded with the oscilloscope were subjected to first-order Butterworth digital filtering: with a low-pass filter with cut-off frequency of 2 GHz chosen so to reduce the effect of noise from the RC and recording systems, and with a high-pass filter with cut-off frequency of 100 kHz chosen to reduce the effect of slow VCSEL power fluctuations.

The FB-loop electronic path includes two Measall KC9601C electrical-signal inverting amplifiers (RFA 1,2, gain band 0.05–10 GHz, gain 20 dB). Since both RFAs are inverting, FB is positive. Between them there are installed: attenuator DYKB DC-6 GHz (ATT) for controlling the FB strength by introducing electronic signal losses; passive equalizer (EQ, introduces fixed losses linearly decreasing from 10 to 0 dB in the range from 0 to 6 GHz) designed for improving the bandwidth uniformity; power divider (RFS 2, identical to RFS 1) for supplying the input signal into the RC system using the Keysight M8195A signal generator with the single-data input time T_S. At the generator output, a 16 dB attenuator (not shown in Fig. 1, *a*) was installed to protect it and restrict the amplitude of signal fed to VCSEL through RFA 2. Paper [9] presents the procedure for forming the RC system input signal from input data relevant to the problem being solved, including the procedure for data masking.

The feedback strength in this system was determined at the point of FB loop opening (corresponding to the ATT output) as the ratio of the signal power fed to RFS 2 to the ATT output signal power. The FB transmission parameters were measured with vector analyzer R&S ZVA40 as the parameter S_{21} modulus. Bandwidth of the entire open loop of the RC system optoelectronic system at the above-defined opening point is determined by the laser modulation bandwidth, which in turn depends on its relaxation oscillation frequency at the preset pump current. In this work we used the VCSEL and SOA pump currents of 3 mA and 83 mA, respectively, at which the open-loop bandwidth was 4.98 GHz at the level of −10 dB from the maximum. Bandwidth of only the electronic part of the path is 0.05–8.9 GHz at the level of −10 dB relative to its maximum bandwidth at the attenuation coefficient belonging to the range of 0–20 dB.

The system's electrical power consumption did not exceed 3.5 W (where 1.17 W is consumed in SOA, 2.25 W — in the entire electronic path, 3.8 mW — in VCSEL); power consumption by the signal generator and oscilloscope was ignored. The FB roundtrip frequency determined from the radio-frequency spectrum is $f_{rep} = 17.2$ MHz (which is consistent with the FB roundtrip time of $\tau = 58$ ns and depends of the time of signal transmission through the optical and electronic paths).

When the FB strength exceeds 0 dB (which matches the ATT attenuation coefficient of 4.5 dB), the system exhibits the Andronov–Hopf bifurcation with the frequency in the vicinity of 4.25 GHz (corresponding to the 247-th harmonic of roundtrip frequency f_{rep}), which evidences high dimensionality of the RC system state space provided by the FB uniformity and large bandwidth. Dynamics observed beyond the bifurcation agrees with that described in [16]: as the attenuation coefficient decreases, the periodic and quasi-periodic modes arise successively.

In the experiments, three sets of parameters were used for different numbers of virtual nodes, which corresponded

Experimental parameters

Parameter	Number of virtual nodes		
	50	100	200
Input signal amplitude, mV	320	320	280
ATT attenuation, dB	5.25	5.25	5.00
Input frequency T_S^{-1}, MHz	64	40	20
T_S, ns	15.6	25	50
τ/T_S	3.72	2.32	1.16

to the best results of solving the considered problem of predicting chaotic time series. The Table presents the values of experimental parameters.

The Santa Fe problem consists in predicting the next time series element based on known values [14] and is more computationally complex than the problem of predicting the Mackey–Glass system dynamics considered in [9]; this requires of the RC system a larger number of nodes and nonlinearity. The prediction error is estimated as the normalized root mean square error (NMSE):

$$\mathrm{NMSE} = \frac{1}{L}\sum_{i=1}^{L}\frac{(Y_i - O_i)^2}{\sigma^2(Y_i)}, \qquad (1)$$

where L is the test sample length, Y_i is the target (true) value of the time series i-th element, O_i is the i-th element value predicted by the system, which is to be obtained by multiplying vector $\mathbf{V}_i$ of the RC system node state values corresponding to the i-th input element by output layer vector $\mathbf{W}$ (see below), i.e. $O_i = \mathbf{V}_i\mathbf{W}$; σ^2 is the dispersion of values.

In the analysis, we used 7000 Santa Fe time series values being sequentially input into the reservoir. Based on the input values and respective vectors of node state values $\mathbf{V}_i$, the train, validation and test samples were formed in accordance with the scheme given in Fig. 2. To prevent overlaps of samples, 500 values between them were excluded from computation.

Fig. 1, *b* presents a case of timing diagrams of the input and output signals for inputting the 2000-th input data value at the parameters taken from the Table 1 (the number of virtual nodes is 100). The system exhibits a response different from the modulation signal, which is caused by nonlinearity in the presence of feedback.

The system training, i.e. selection of the output layer vector weights $\mathbf{W}$, was performed via the Tikhonov regularization which is a generalized linear regression

$$\mathbf{W} = (\mathbf{M}^T\mathbf{M} + \lambda\mathbf{I})^{-1}\mathbf{M}^T\mathbf{Y}_{train}, \qquad (2)$$

Here $\mathbf{Y}_{train}$ is the vector of target values on the train sample, matrix $\mathbf{M}$ is composed of vectors $\mathbf{V}_i$ of the reservoir node state values on the train sample, $\mathbf{I}$ is the unity matrix of the appropriate dimension, λ is the low-value regularization parameter which was selected using single-parameter optimization consisting in minimizing NMSE on the validation sample.

To reduce NMSE by increasing the RC system state space and nonlinearity, there was proposed [17] a processing procedure involving concatenation of the node state values vector $\mathbf{V}_i$ with its squared components, i.e. obtaining vector $\mathbf{V}_i^{sq} = [\mathbf{V}_i; \mathbf{V}_i^2]$. In our experiments, we used a new procedure for processing node state values, which consists in utilizing a nonlinear sigmoid function tanh to obtain values $\mathbf{V}_i^{th} = \tanh(k\mathbf{V}_i)$, where k is selected on a validation sample, and multiplication by k, as well as calculation of the tanh function, is performed element-by-element. Vector $\mathbf{V}_i$ is preliminary normalized to the $[-1, 1]$ range. Normalized values of this vector are calculated as $2\big((\mathbf{V}_i - V_{\min})/V_{\max} - 0.5\big)$, where normalization coefficients $V_{\min} = \min(\mathbf{V}_i)$ and $V_{\max} = \max(\mathbf{V}_i - V_{\min})$ are selected on the $\mathbf{V}_i$ vectors corresponding to the train sample and then fixed. In addition, there was used a modified procedure proposed in [17], that is, successive application of function tanh to the concatenation results, i.e., $\mathbf{V}_i^{sq,th} = \tanh(k\mathbf{V}_i^{sq})$.

Thus, in solving the problem of predicting time series, construction of matrix $\mathbf{M}$ for calculating $\mathbf{W}$ (equation (2)) and determination of output O_i will be performed by using either node state values $\mathbf{V}_i$ (procedure *A*) or modified state vectors $\mathbf{V}_i^{sq}$ (procedure *B*), $\mathbf{V}_i^{th}$ (procedure *C*), $\mathbf{V}_i^{sq,th}$ (procedure *D*).

Fig. 3 presents NMSE values used in experimentally solving the Santa Fe problem, which were obtained via different procedures for node states processing. The figure shows the mean values and standard deviations obtained from five repetitions of measurements. Low relative standard deviation (not higher than 5.8 %) evidences good reproducibility of experimental results and consistency of the RC system.

Data presented in Fig. 3 show that the lowest NMSE value in the absence of additional processing (procedure *A*) is 0.16 (for 100 nodes). Increasing the number of nodes jointly with increasing the input time of a single data element

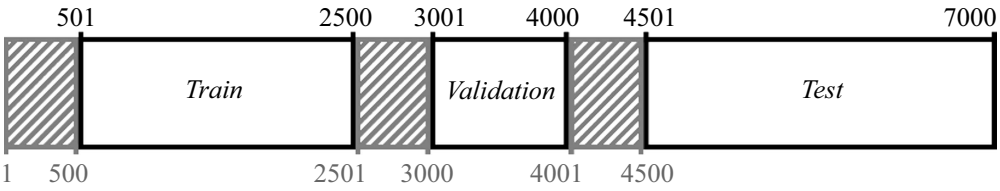

Figure 2. The scheme of forming samples from arrays of input data and respective vectors of node state values depending on serial number. The grey-shaded areas correspond to unused values.

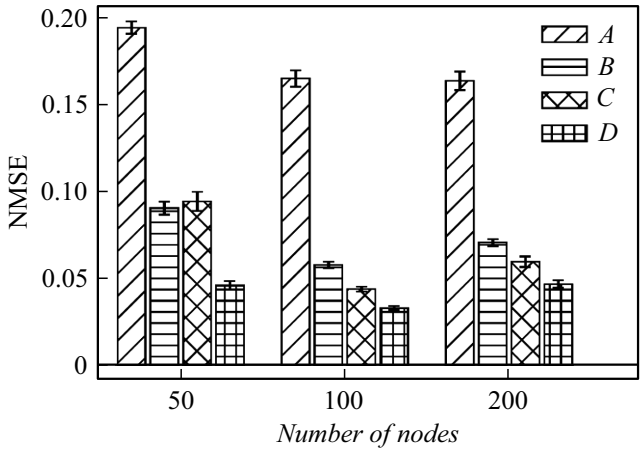

Figure 3. NMSE in solving the Santa Fe problem for different numbers of nodes and different procedures for processing the node values.

does not improve the results, which agrees well with the results presented in [18], where it was shown that, for the long-delay RC systems where τ significantly exceeds the system response time, it is reasonable to reduce the problem solution errors by using several symbol inputs in one resonator roundtrip, i.e. $\tau/T_S \geqslant 2$.

When additional processing is used (procedures B, C, D), a significant reduction in NMSE is observed in all the cases. Therewith, the method involving the nonlinear function tanh (procedure C) has an advantage over concatenation with squared state vector components (procedure B) for 100 and 200 nodes. The hybrid method combining the nonlinear function and concatenation with squared values (procedure D) exhibits the lowest error amounting to 0.046, 0.033 and 0.047 for 50, 100 and 200 nodes, respectively, which is comparable with the results presented in [13,19] (0.022 and 0.045). The maximum achievable processing speed of the system under consideration (64 Msamples/s at the input frequency of 64 MHz) exceeds 1 and 24.5 Msamples/s for the RC systems presented in [13,19].

Thus, by modifying the output layer it is possible to improve the quality of the RC system solutions without complicating the training process, that is, selection of weighting factors **W** which, as previously, are being determined by the Tikhonov regularization.

Note in conclusion that this study has experimentally demonstrated the operation of optoelectronic RC system based on VCSEL and semiconductor optical amplifier in solving the problem of predicting Santa Fe chaotic time series; various methods for processing virtual node state values have been analyzed. The study has shown that the use of output layer employing the processing procedure consisting in sequentially applied concatenation of the vector of RC system node state values with the vector of their squares and calculation of nonlinear function tanh can significantly reduce the error in the Santa Fe problem solutions, namely to 0.033 at the data input frequency of 40 MHz (corresponding to the processing speed of 40 Msamples/s). Taking into account the latest achievements in the field of analog optoelectronic computing [20], it is possible to form the output layer and implement the procedure for processing the virtual node state values in the analog form with an increase in the computation energy efficiency and speed, which makes promising this area of research.

Funding

The study was supported by the Russian Science Foundation, project No 23-72-01050 (https://rscf.ru/project/23-72-01050/).

Conflict of interests

The authors declare that they have no conflict of interests.

References

[1] L. Appeltant, M.C. Soriano, G. Van der Sande, J. Danckaert, S. Massar, J. Dambre, B. Schrauwen, C.R. Mirasso, I. Fischer, Nat. Commun., **2**, 468 (2011). DOI: 10.1038/ncomms1476
[2] J.D. Hart, L. Larger, T.E. Murphy, R. Roy, Phil. Trans. Roy. Soc. A, **377** (2153), 20180123 (2019). DOI: 10.1098/rsta.2018.0123
[3] M. Yan, C. Huang, P. Bienstman, P. Tino, W. Lin, J. Sun, Nat. Commun., **15** (1), 2056 (2024). DOI: 10.1038/s41467-024-45187-1
[4] S. Abreu, I. Boikov, M. Goldmann, T. Jonuzi, A. Lupo, S. Masaad, L. Nguyen, E. Picco, G. Pourcel, A. Skalli, L. Talandier, B. Vettelschoss, E.A. Vlieg, A. Argyris, P. Bienstman, D. Brunner, J. Dambre, L. Daudet, J.D. Domenech, I. Fischer, F. Horst, S. Massar, C.R. Mirasso, B.J. Offrein, A. Rossi, M.C. Soriano, S. Sygletos, S.K. Turitsyn, Rev. Phys., **12**, 100093 (2024). DOI: 10.1016/j.revip.2024.100093
[5] X. Liang, J. Tang, Y. Zhong, B. Gao, H. Qian, H. Wu, Nat. Electron., **7** (3), 193 (2024). DOI: 10.1038/s41928-024-01133-z
[6] X. Shi, L.L. Minku, X. Yao, IEEE Trans. Comput., **71** (110), 2766 (2022). DOI: 10.1109/TC.2022.3173151
[7] W. Namiki, D. Nishioka, Y. Yamaguchi, T. Tsuchiya, T. Higuchi, K. Terabe, Adv. Intell. Syst., **5** (12), 2300228 (2023). DOI: 10.1002/aisy.202300228
[8] G. Abdi, T. Mazur, K. Szaciłowski, Jpn. J. Appl. Phys., **63** (5), 50803 (2024). DOI: 10.35848/1347-4065/ad394f
[9] G.O. Danilenko, D.A. Pavlov, E.A. Viktorov, A.V. Kovalev, Tech. Phys. Lett., **50** (9), 24 (2024). DOI: 10.61011/TPL.2024.09.59147.19971.
[10] P.S. Dmitriev, A.V. Kovalev, A. Locquet, D. Rontani, E.A. Viktorov, Opt. Lett., **45** (22), 6150 (2020). DOI: 10.1364/OL.405177
[11] G.O. Danilenko, A.V. Kovalev, E.A. Viktorov, A. Locquet, D.S. Citrin, D. Rontani, Chaos, **33** (1), 013116 (2023). DOI: 10.1063/5.0127661

[12] G.O. Danilenko, A.V. Kovalev, E.A. Viktorov, A. Locquet, D.S. Citrin, D. Rontani, Chaos, **33** (11), 113125 (2023). DOI: 10.1063/5.0172039
[13] B.H. Klimko, Y.K. Chembo, IEEE Photon. Technol. Lett., **36** (23), 1353 (2024). DOI: 10.1109/LPT.2024.3477352
[14] A.S. Weigend, N.A. Gershenfeld, *Time series prediction: forecasting the future and understanding the past* (Routledge, N.Y., 1993).
[15] A. Ohkubo, M. Inubushi, Sci. Rep., **14**, 30918 (2024). DOI: 10.1038/s41598-024-81880-3
[16] M.S. Islam, A.V. Kovalev, G. Coget, E.A. Viktorov, D.S. Citrin, A. Locquet, Phys. Rev. Appl., **13** (6), 064038 (2020). DOI: 10.1103/PhysRevApplied.13.064038
[17] J. Pathak, B. Hunt, M. Girvan, Z. Lu, E. Ott, Phys. Rev. Lett., **120**, 024102 (2018). DOI: 10.1103/PhysRevLett.120.024102
[18] K. Saito, K. Kanno, A. Uchida, Nonlin. Theory Appl., **15**, 764 (2024). DOI: 10.1587/nolta.15.764
[19] I. Estèbanez, A. Argyris, I. Fischer, Opt. Lett., **48** (9), 2449 (2023). DOI: 10.1364/OL.485545
[20] Z. Lin, B.J. Shastri, S. Yu, J. Song, Y. Zhu, A. Safarnejadian, W. Cai, Y. Lin, W. Ke, M. Hammood, T. Wang, M. Xu, Z. Zheng, M. Al-Qadasi, O. Esmaeeli, M. Rahim, G. Pakulski, J. Schmid, P. Barrios, W. Jiang, H. Morison, M. Mitchell, X. Guan, N.A.F. Jaeger, L.A. Rusch, S. Shekhar, W. Shi, S. Yu, X. Cai, L. Chrostowski, Nat. Commun., **15**, 9081 (2024). DOI: 10.1038/s41467-024-53261-x

Translated by EgoTranslating